ICROS-SICE International Joint Conference 2009
August 18-21, 2009, Fukuoka International Congress Center, Japan

Observation of Human Multi-Joint Arm Movement from the Viewpoint of a Riemannian Distance

Masahiro Sekimoto[1], Suguru Arimoto[1,2], Boris I. Prilutsky[3], Tadao Isaka[1,4], and Sadao Kawamura[1,4]

[1]Research Organization of Science and Engineering, Ritsumeikan University, Kusatsu, Japan
(Tel: +81-77-561-4910; E-mail: sekimoto@fc.ritsumei.ac.jp)
[2]RIKEN-TRI Collaboration Center, RIKEN, Nagoya, Japan
[3]Center for Human Movement Studies, Georgia Institute of Technology, Atlanta, Georgia, USA
[4]Department of Robotics, Ritsumeikan University, Kusatsu, Japan

Abstract: This paper aims at analyzing dynamic characteristics of human arm movements from the viewpoint of Riemannian distance. In order to evaluate the amount of inertia-induced movement of a multi-joint arm, a measure called inertia-induced measure is developed. By applying the measure to actual human reaching, it is shown that the smooth reaching tends to be closer to the inertia-induced movement than the clumsy reaching. From this observation, it is suggested that humans use their own inertia properties efficiently in smooth reaching.

Keywords: Inertia-induced movement, Motion analysis, Human reaching, Riemannian distance, Dynamics

1. INTRODUCTION

Humans and robots constitute a common structure: a series of links that are connected through rotational joints. During fast movements of such a multi-body system, inertia-induced effects (*i.e.*, inertia, centrifugal, and Coriolis forces) are dominant except for robots with high gear-ratio joints, and Lagrange's equation of motion for this multi-body system becomes intrinsically nonlinear. A particle moves straight with no acceleration when there is no external force or the sum of forces acting on the particle is zero; this is generally known as the law of inertia. In contrast, physical characteristics of motion of a multi-body system in such a case have not yet been shown explicitly. Very recently, it has been demonstrated that inertia-induced movement of a multi-body system is characterized by a geodesic curve corresponding to a Riemannian distance in a Riemannian manifold [1].

A Riemannian distance is a technical term used in Riemannian geometry which is an important branch of differential geometry. The traditional Riemannian geometry focuses on a broad range of geometries whose metric properties vary from point to point. Three decades ago (1978), Arnold [2] noticed the importance of Riemannian geometry in modeling, analysis, and control of mechanical systems. Recently, Bullo and Lewis [3] have shown that an equation of motion of a multi-body system can be treated using Riemannian geometry. Thus, Riemannian geometry can also deal with movement of a multi-body system. Arimoto [4], introducing the ideas of Riemannian geometry in Robotics independently of Bullo and Lewis's work, has shown that given a robot as a multi-body mechanism with n degrees-of-freedom (DOFs) and the free endpoint, the set of its all postures can be regarded as a Riemannian manifold (M, g) associated with the Riemannian metric g that constitutes the robot's inertia matrix. On the basis of this fact, Arimoto *et al.* [5] have suggested the new movement stability analysis (the nonlinear closed-loop dynamics analysis) of a multi-joint robot arm with joint redundancy when the passivity based control was applied to the system. Then, a geodesic connecting any two postures with the Riemannian distance corresponds to an orbit expressed in a local coordinate chart and generated by a solution to the Euler-Lagrange equation of robot motion originating only from inertia-induced force [1]. Furthermore, the Riemannian-geometry viewpoint has been extended to an important class of dynamics of multi-body systems physically interacting with an object or with environment through holonomic or/and nonholonomic (but Pfaffian) constraints [5].

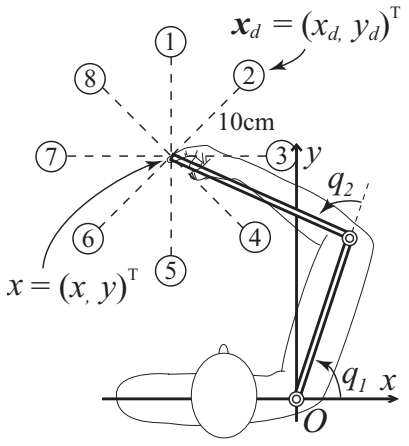

Fig. 1 Planar movement of a human upper arm with two joints

Aside from movements of a multi-joint robot, human multi-body movements have attracted a lot of attention and various studies have been conducted. The widely known features of human skilled reaching by the arm are a straight endpoint trajectory and a bell-shaped endpoint velocity profile [6]. A lot of studies of human movement including the above observations have focused on the kinematic properties. However, fewer studies have dealt with dynamics due to lack of mathematical tools for analyzing dynamic characteristics of human movements.

PR0002/09/0000-2664 ¥400

This paper aims at analyzing dynamic characteristics of human arm reaching movements from the viewpoint of Riemannian distance. In particular, this paper focuses on how humans cope with dynamics of their own arms during reaching. In order to analyze the role of arm inertial properties in human movement, a measure for evaluating the amount of inertia-induced movement of a multi-joint arm, called *an inertia-induced measure*, is proposed. The inertia-induced measure was used to analyze human planar reaching. It is shown that in smooth reaching, the calculated inertia-induced measure profile has peaks at the initial and final stages of motion and the measure values are small during other stages of motion. However, the values of the inertia-induced measure are relatively large in general in clumsy reaching. Based on these observations, it is suggested that humans use their own inertia properties efficiently in smooth reaching.

2. RIEMANNIAN DISTANCE: INERTIA-INDUCED MOVEMENT OF A MULTI-JOINT SYSTEM

Let us consider a multi-joint system with n rigid bodies connected in series through rotational joints as shown in Fig.1. If a posture of the system is represented by p, the set of all such possible postures M and a family of subsets of M can be determined naturally. Since the set M becomes Hausdorff and compact as far as the object is confined to multi-joint systems existing in the real world, the set M with such a family of open subsets can be regarded as a differentiable manifold of class C^∞ [7]. Furthermore, every point p of M has a neighborhood U that is homeomorphic to an open subset Ω of n-dimensional numerical space $\mathbf{R}^n$ constructed by local coordinates $(q_1, \ldots, q_n)$, and such a homeomorphism $(\phi : \mathrm{U} \to \Omega)$ is called a coordinate chart. As the local coordinates, it is reasonable to choose generalized coordinates of the system, that is, the joint angles given in $q_i \in (-\pi, \pi]$ $(i = 1, \ldots, n)$ as defined in Fig.1.

Next, let I be an interval $(-\varepsilon, \varepsilon)$ and define a curve $c(t)$ by a mapping $c : I \to M$ such that $c(0) = p$. If for any given curve $\bar{c}$ a relation $(\sim)$ is defined by

$$c \sim \bar{c} \Longleftrightarrow \frac{\mathrm{d}(\phi \circ c)}{\mathrm{d}t}(0) = \frac{\mathrm{d}(\phi \circ \bar{c})}{\mathrm{d}t}(0) \tag{1}$$

in a coordinate chart (U, ϕ) around p, then it becomes the equivalence relation, and the equivalence class of curves $c : I \to M$ is called a tangent vector to M at p. This definition of tangent vectors to M at p does not depend on choice of the coordinate chart at p, as discussed in the textbooks [8, 9]. Furthermore, the set of all tangent vectors to M at p is denoted by T_pM and called the tangent space at $p \in M$. It has an n-dimensional linear space structure like $\mathbf{R}^n$.

Now, for a given $n \times n$ symmetric positive definite matrix $G(c(t))$ whose (i, j)-entry is denoted by g_{ij}, define a Riemannian metric in the differentiable manifold (M, p) as a mapping $g_p : T_pM \times T_pM \to \mathbf{R}$ such that $p \to g_p$ is of class C^∞ and, for $u = u^i(\partial/\partial q_i) \in T_pM$ and $v = v^i(\partial/\partial q_i) \in T_pM$, $g_p(u, v)$ is a symmetric positive definite quadratic form:

$$g_p(u, v) = \sum_{i,j=1}^{n} g_{ij}(p) u^i v^j \tag{2}$$

Then, the manifold (M, p) can be regarded as a connected Riemannian manifold and becomes complete as a metric space. Hence, it is possible to define a length of $c(t) \in M$ to be

$$L(c(t)) = \int_a^b \|\dot{c}(t)\| \mathrm{d}t = \int_a^b \sqrt{g_{c(t)}(\dot{c}(t), \dot{c}(t))}\, \mathrm{d}t \tag{3}$$

Then, since any connected Riemannian manifold becomes a metric space whose induced topology is coincident with the given manifold topology, it is also possible to define a Riemannian distance $d(p, p')$ for any pair of points $p, p' \in M$ as the infimum of all admissible curves from p to p' as follows:

$$d(p, p') = \inf L(c(t)) \tag{4}$$

As described in the textbooks on Riemannian geometry [8, 9], an admissible curve c in a Riemannian manifold is said to be minimizing if $L(c) \leq L(\tilde{c})$ for any other admissible curve $\tilde{c}$ with the same endpoints. It follows immediately from the definition of distance that c is minimizing if and only if $L(c)$ is equal to the distance between the endpoints. Furthermore, it is known that if the Riemannian manifold (M, g) is complete then for any pair of points p and p' there exists at least a minimizing curve $c(t)$, $t \in [a, b]$, with $c(a) = p$ and $c(b) = p'$. If such a minimizing curve $c(t)$ is described with the aid of coordinate chart (U, ϕ) as $\phi(c(t)) = (q_1(t), \cdots, q_n(t))(= q(t))$ then it satisfies the 2nd-order differential equation:

$$\ddot{q}_k(t) + \sum_{i,j=1}^{n} \Gamma_{ij}^k(q(t)) \dot{q}_i(t) \dot{q}_j(t) = 0 \qquad (k = 1, \cdots, n) \tag{5}$$

where Γ_{ij}^k denotes Christoffel's symbol defined by

$$\Gamma_{ij}^k = \frac{1}{2} \sum_{h=1}^{m} g^{kh} \left(\frac{\partial g_{ih}}{\partial q_j} + \frac{\partial g_{jh}}{\partial q_i} - \frac{\partial g_{ij}}{\partial q_h} \right) \tag{6}$$

and (g^{kh}) denotes the inverse of matrix (g_{kh}). A curve $q(t) : I \to U$ satisfying eq.(5) together with $\phi^{-1}(q(t))$ is called a geodesic and eq.(5) itself is called a geodesic equation. Furthermore, the geodesic equation of eq.(5) can be transformed, by multiplying eq.(5) from the left-hand by (g_{ki}), into

$$g_{ki}\ddot{q}_i(t) + \sum_{i,j=1}^{n} \Gamma_{ikj}(q(t)) \dot{q}_i(t) \dot{q}_j(t) = 0 \qquad (k = 1, \cdots, n) \tag{7}$$

where Γ_{ikj} denotes another Christoffel's symbol defined by

$$\Gamma_{ikj} = \frac{1}{2} \left(\frac{\partial g_{ik}}{\partial q_j} + \frac{\partial g_{jk}}{\partial q_i} - \frac{\partial g_{ij}}{\partial q_k} \right) \tag{8}$$

Meanwhile, in mechanics and robotics, Lagrange's equation of motion of the multi-joint arm [10] is described by:

$$H(\boldsymbol{q}(t))\ddot{\boldsymbol{q}}(t) + \left\{\frac{1}{2}\dot{H}(\boldsymbol{q}(t)) + S(\boldsymbol{q}(t), \dot{\boldsymbol{q}}(t))\right\}\dot{\boldsymbol{q}}(t) = \boldsymbol{u}(t) \quad (9)$$

where $\boldsymbol{q}(t) = (q_1(t), \ldots, q_n(t))^{\mathrm{T}}$ denotes the vector of joint angles, $H(\boldsymbol{q}(t))$ the inertia matrix, $S(\boldsymbol{q}(t), \dot{\boldsymbol{q}}(t))\dot{\boldsymbol{q}}(t)$ the gyroscopic force term including centrifugal and Coriolis forces, $S(\boldsymbol{q}(t), \dot{\boldsymbol{q}}(t))$ the skew-symmetric matrix, $\boldsymbol{u}$ the control input torque at joints. The inertia matrix $H(\boldsymbol{q}(t))$ is symmetric and positive definite. Furthermore, each entry h_{ij} of $H(\boldsymbol{q}(t))$ is a constant or a sinusoidal function of components of joint angle vector $\boldsymbol{q}(t)$. Hence, $H(\boldsymbol{q}(t))$ is symmetric, positive definite and differentiable of class C^{∞}.

Now, suppose that the inertia matrix h_{ij} of the system is chosen as g_{ij} in the Riemannian metric defined by eq.(2), *i.e.,* $g_{ij} = h_{ij}$ for $i, j = 1, \ldots, n$. Then, the left-hand side of the geodesic equation of eq.(7) is coincident with that of the system dynamics of eq.(9) because by referring to the book [10] and the paper [7] it satisfies

$$\left\{\frac{1}{2}\dot{H}(\boldsymbol{q}) + S(\boldsymbol{q}, \dot{\boldsymbol{q}})\right\}\dot{\boldsymbol{q}} = \sum_{i,j=1}^{n} \Gamma_{ikj}(q)\dot{q}_i\dot{q}_j \quad (10)$$

Hence, the system dynamics with $\boldsymbol{u} = 0$ is coincident with the geodesic equation [7]. This means that if an inertia matrix of system is chosen as g_{ij} in the Riemannian metric of eq.(2) then a geodesic $q(t)$ represents a motion from $q(a) = p$ to $q(b) = p'$ over an interval $t \in [a, b]$ without input torques in the physical sense, that is, inertia-induced movement (pure inertia, Coriolis, and centrifugal forces movement) of a multi-joint system. Furthermore, the Riemannian distance itself, which is the minimum in lengths determined by eq.(3) of all possible motions from a posture $p(= q(a))$ to another $p'(= q(b))$, corresponds to inertia-induced movement of a multi-joint system. Note that a Riemannian distance itself is invariant even if for given positive constants α and β the subsidiary variable t is replaced with $s = \alpha t + \beta$, that is, it depends only on the endpoints p and p' in the Riemannian manifold as discussed in the textbooks [8, 9].

3. INERTIA-INDUCED MEASURE

As described in the previous section, a length in eq.(3) based on a Riemannian metric with a system inertia matrix represents the amount of inertia-induced movement of a multi-joint system. For some multi-joint movement from a posture $p(= q(a))$ to another posture $p'(= q(b))$, if the motion is far from the inertia-induced movement (the geodesic orbit obtained by eq.(5) or (7)), the trajectory length is longer than the Riemannian distance between the points p and p'. On the other hand, if the motion is similar to the geodesic orbit, the trajectory length is close to the Riemannian distance. Note that a length of any admissible curve c between p and p' in a Riemannian manifold is more than or equal to a corresponding Riemannian distance, *i.e.,* $L(c) \geq d(p, p')$. Hence, a length of eq.(3) together with a Riemannian distance of eq.(4) based on a system inertia matrix is available to evaluate the amount of inertia-induced movement of a multi-joint system.

In general, dynamics of an actual human or robot differ from the ideal dynamics shown by eq.(9) and contain viscoelastic, Coulomb friction, and gravity forces. An equation of motion of such complicated system can be described by

$$H(\boldsymbol{q})\ddot{\boldsymbol{q}} + \left\{\frac{1}{2}\dot{H}(\boldsymbol{q}) + S(\boldsymbol{q}, \dot{\boldsymbol{q}})\right\}\dot{\boldsymbol{q}} + C\dot{\boldsymbol{q}} + K\Delta\boldsymbol{q} + \boldsymbol{f}_c + \boldsymbol{g}(\boldsymbol{q}) = \boldsymbol{u} \quad (11)$$

where $C\dot{\boldsymbol{q}}$ denotes joint viscosities, $K\Delta\boldsymbol{q}$ denotes joint elastics, $\boldsymbol{f}_c$ denotes a Coulomb friction, $\boldsymbol{g}(\boldsymbol{q})$ denotes the gravity effect. Even in the case of such complicated dynamics it is possible to evaluate the amount of inertia-induced movement of the system. Now, we focus on some interval $t \in [a, b]$ during the motion governed by the dynamics of eq.(11) with $\boldsymbol{u} = \boldsymbol{0}$. For a measured orbit of state variables of a system, a length corresponding to the motion within $[a, b]$ can be calculated by applying the motion data to eq.(3) or the following expression

$$L = \int_a^b \sqrt{\dot{\boldsymbol{q}}(t)^{\mathrm{T}} H(\boldsymbol{q}(t))\dot{\boldsymbol{q}}(t)}\, \mathrm{d}t \quad (12)$$

On the other hand, the corresponding Riemannian distance between the postures $\boldsymbol{q}(a)$ and $\boldsymbol{q}(b)$ is available from eq.(4). In more detail, the Riemannian distance can be obtained by solving the two-point boundary value problem under the geodesic equation of eq.(5) or (7) together with the two boundary conditions $\boldsymbol{q}(a)$ and $\boldsymbol{q}(b)$ and applying the obtained geodesic orbit to eq.(12). Thus, it is possible to evaluate the inertia-induced amount of the target motion by comparing the obtained length with the corresponding Riemannian distance. However, the evaluated motion must be far from the inertia-induced movement because the other forces except the inertia-induced force are exerted on the system. As another situation, we consider the case that a control input torque

$$\boldsymbol{u} = C\dot{\boldsymbol{q}} + K\Delta\boldsymbol{q} + \boldsymbol{f}_c + \boldsymbol{g}(\boldsymbol{q}) \quad (13)$$

is applied to the system so as to cancel the forces except the inertia-induced force. In this case, the calculated length must be close to the Riemannian distance, hence, the evaluated motion should be close to the inertia-induced movement. Thus, even if other forces except the inertia-induced force are exerted on the system, it is possible to evaluate the amount of inertia-induced movement of a multi-joint system. This is physically reasonable given an analogy with a particle motion under action of external forces.

Now, we suggest a measure to evaluate the amount of inertia-induced movement of a multi-joint system on the basis of physical properties of the Riemannian distance, called *inertia-induced measure*. For an interval $t \in [a, b]$ arbitrarily set within movement, the measure is defined by

$$R = L - d(\boldsymbol{q}(a), \boldsymbol{q}(b)) \quad (14)$$

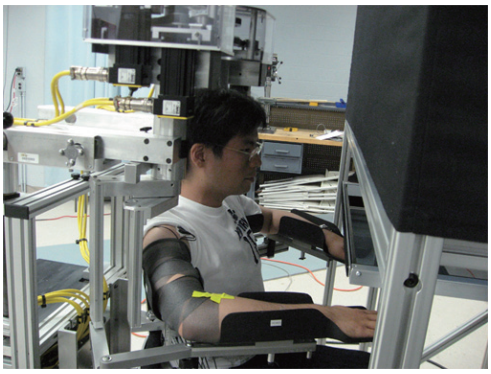

Fig. 2 An experimental setup

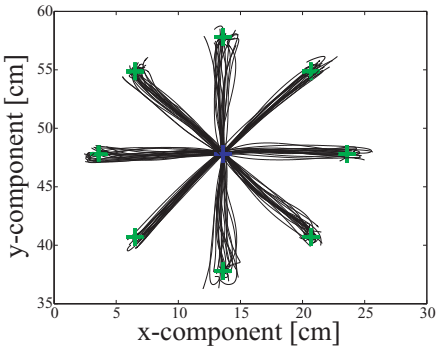

Fig. 3 Endpoint trajectories of 20 trials

where L denotes the length defined by eq.(12) and $d(\boldsymbol{q}(a), \boldsymbol{q}(b))$ denotes the Riemannian distance defined by eq.(4) between the postures $\boldsymbol{q}(a)$ and $\boldsymbol{q}(b)$. When the motion is exactly equal to the inertia-induced movement, the measure shows $R = 0$, while the measure has the large values when the target motion is far from the inertia-induced movement. Furthermore, we suggest the normalized measure defined by

$$R_N = (L - d(\boldsymbol{q}(a), \boldsymbol{q}(b))) \,/\, d(\boldsymbol{q}(a), \boldsymbol{q}(b)) \qquad (15)$$

It is possible to set the interval $t \in [a, b]$ according to user's demands. If transient effects are of interest, a small interval should be set. However, if the inertia-induced amount of motion is investigated over an entire movement, the movement onset and offset times should be set as the interval.

4. OBSERVATION OF REACHING FROM THE VIEWPOINT OF RIEMANNIAN DISTANCE

In order to investigate dynamic properties in human reaching from the viewpoint of the inertia-induced measure, human planar reaching experiments were conducted as shown in Fig.1. Figure 2 demonstrates an experimental setup for reaching experiments using a robotic system Kinarm (BKIN Technologies, Canada). The subject was sitting in a Kinarm chair with the arms resting on two-joint robotic arms in the horizontal plane (see the paper by Scott [11] for Kinarm description). The chair and the robotic arm were adjusted so that the subject could move the arms in the horizontal plane at a chest level. The subject was instructed to reach as fast and accurately as possible one of 8 targets, which appeared randomly on the horizontal screen in front of the subject, with the index finger tip of right hand. The targets were circles of 1 [cm] in diameter arranged radially around the start position 10 [cm] away from it. When the target was reached, the color of target was changed so that the subject could assess if the task was successfully accomplished. It disappeared within 1 [s] of "touch" and the subject moved the arm back to the initial (center) position and waited for a next target to appear. After reaching all 8 targets in random order (one trial), next trials of reaching movements were performed until 20 trials were completed. The Kinarm is capable of generating a force field imposed on the arm through the motor-actuated torques applied at the shoulder and elbow joints, but this function was not used in the experiment. Figure 3 depicts endpoint trajectories of all 20 trials of one subject. The joint angles and angular velocities of the arm were measured by the encoders built in the robotic arm of Kinarm. The endpoint position shown in Fig.3 was calculated from the kinematic information of the arm: subject's segment lengths and the joint angles.

Table 1 The arm parameters of the subject

Link number	1	2
Length [m]	0.2780	0.4080
Center of mass [m]	0.1498	0.1456
Mass [kg]	2.001	1.621
Inertia moment [kgm^2]	1.023×10^{-2}	1.951×10^{-2}

The evaluation of the inertia-induced measure was conducted by using the obtained data. First, each movement was divided into 30 segments according to movement time. Next, for each interval the length of eq.(12) and the Riemannian distance were calculated from the data according to the procedure described in Section 3. Finally, the values of the inertia-induced measure as described by eqs.(14) and (15) were calculated by using the calculated length and the Riemannian distance. These steps were repeated for all 30 segments to obtain the profiles of the inertia-induced measure. The inertia matrix of human arm required for the calculation of the length and the Riemannian distance, *i.e.,* the link inertias and link mass, was estimated by referring to the book [12]. Table 1 shows the estimated arm parameters of the subject.

Figures 4 and 5 depict two typical results observed in the experiment. Figure 4 shows mechanical characteristics of reaching to target 2 in trial 13; Figure 5 shows the same characteristics for trial 18. Each figure presents the endpoint trajectory, the estimated kinetic energy profile, the joint angle profile, the angular velocity profile, the profile of the inertia-induced measure defined by eq.(14), and the profile of the normalized measure defined by eq.(15). The kinetic energy was calculated on the basis of the estimated inertia matrix. It can be seen that the motion in Fig.4 becomes clumsy around the target (*i.e.*, the path curvature sharply changed). On the other hand, a smooth reaching movement is observed in Fig.5, al-

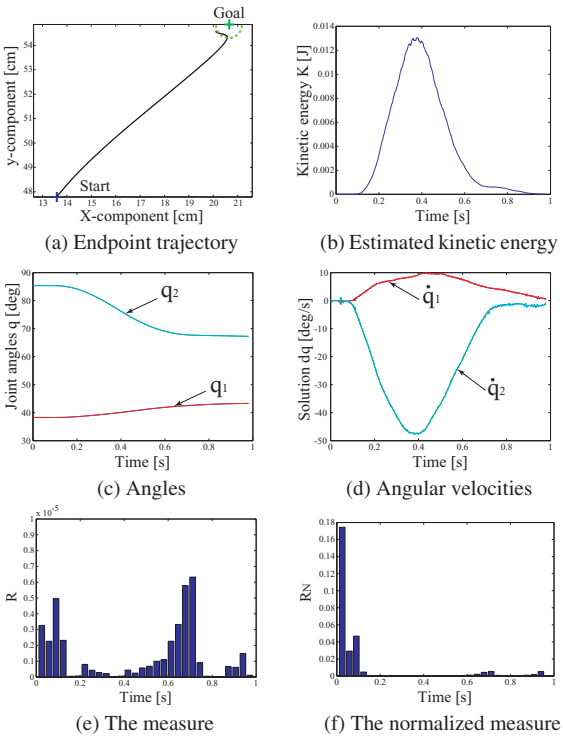

(a) Endpoint trajectory (b) Estimated kinetic energy
(c) Angles (d) Angular velocities
(e) The measure (f) The normalized measure

Fig. 4 Experimental results in the case of clumsy reaching

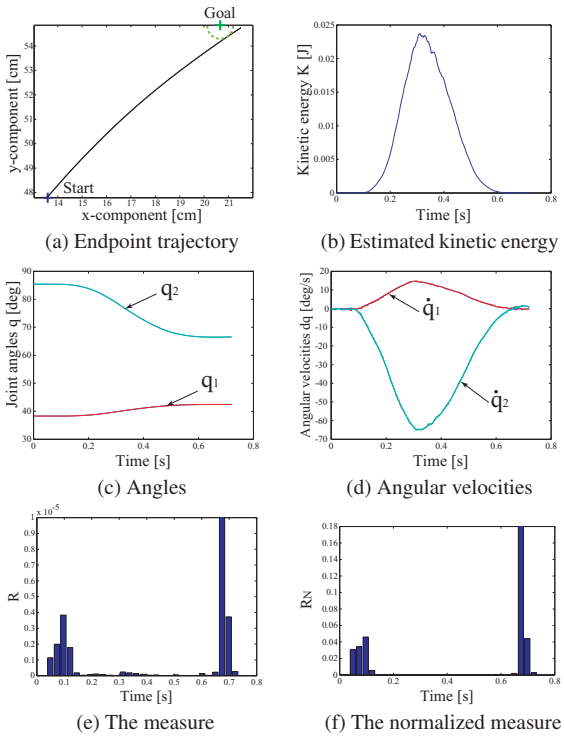

(a) Endpoint trajectory (b) Estimated kinetic energy
(c) Angles (d) Angular velocities
(e) The measure (f) The normalized measure

Fig. 5 Experimental results in the case of smooth reaching

though the end-point did not reach the target and passed very close to it. The fact that the target was missed in trial 18 does not present a problem since our concern in the paper is the application of the inertia-induced measure analysis to human reaching rather than the reaching performance. The profiles of the non-normalized and normalized inertia-induced measure show that the values tend to be large around the initial and final stages of movement. As discussed in Section 3, the quantity R becomes small when the observed movement is close to the inertia-induced movement and large when it is far from it. Hence, it appears that the large R values coincide with subject's attempts to initiate or stop the arm at these movement phases. In particular, during the clumsy reaching, the subject attempted to move the arm and correct its trajectory so as to reach the target at the final stage of motion. The inertia-induced measure represents this behavior by large R values in Fig.4(e). On the other hand, the results show that the R values tend to be relatively small during other movement stages (e.g., middle stage) especially if reaching is smooth (Figs.4 and 5). Based on these results it can be suggested that humans take into account their own inertia properties and use them efficiently during fast reaching motion.

The inertia-induced measure can also provide the amount of inertia-induced movement over an entire reaching motion by setting boundary conditions at the start and end of motion. The overall amount of inertia-induced movement was $R_N = 10.1[\%]$ in the clumsy reaching, and $R_N = 1.07[\%]$ in the smooth reaching. These results clearly illustrate the difference in dynamic properties between the two reaching movements. As discussed in Section 3, the length of eq.(12) depends not only on the initial and final postures of the reaching motion within a predefined time interval, but also on movement time. In contract, the Riemannian distance depends only on the initial and final postures, regardless of movement time. Hence, the normalized R measure can be useful for comparing movements with different speed and different Riemannian distance.

5. CONCLUSIONS

The inertia-induced measure was proposed to evaluate the amount of inertia-induced movement of a multi-joint system, and dynamic properties of human reaching were analyzed by using this measure. An important benefit of the measure is that it allows for analysis of inertia-induced movement of a multi-joint system. The inertia-induced measure can be used to evaluate the amount of inertia-induced motion for variety of multi-joint movements. The analysis can be used when a motion is subject to gravity and external forces as long as the motion is primarily governed by an inertia-induced force. Hence, we plan to apply the inertia-induced measure to analyses of other movements (for instance, human walking) in future work.

ACKNOWLEDGMENTS

This work was partially supported by KAKENHI (No.20760175): Grant-in-Aid for Young Scientists (B) of the MEXT, Japan. The authors thank Ms. Linda Harley and Mr. Gregory Philips of Georgia Institute of Tech-

nology, USA, for their help in data collection. Also, the authors thank Dr. Takahiro Wada of Kagawa University, Japan, for valuable discussions.

REFERENCES

[1] M. Sekimoto, S. Arimoto, S. Kawamura, and J.-H. Bae, "Skilled-motion plannings of multi-body systems based upon Riemannian distance," in *Proc. of the 2008 IEEE International Conference on Robotics and Automation (ICRA2008)*, Pasadena, CA, May 19-23 2008, pp. 1233–1238.

[2] V. I. Arnold (Trs. K. Vogtmann and A. Weinstein), *Mathematical methods of classical mechanics (2nd ed.)*. New York: Springer-Verlag, 1989.

[3] F. Bullo and A. D. Lewis, *Geometric Control of Mechanical Systems: Modeling, Analysis, And Design For Simple Mechanical Control Systems*. Springer, New York, 2000.

[4] S. Arimoto, "Modelling and control of multi-body mechanical systems Part I: A Riemannian geometry approach," *International Journal of Factory Automation, Robotics and Soft Computing*, 2009, (in press).

[5] S. Arimoto, M. Yoshida, M. Sekimoto, and K. Tahara, "A Riemannian-geometry approach for control of robotic systems under constraints," *SICE Journal of Control, Measurement, and System Integration*, vol. 2, no. 2, pp. 107–116, Mar. 2009.

[6] P. Morasso, "Spatial control of arm movements," *Experimental Brain Research*, vol. 42, no. 2, pp. 223–227, 1981.

[7] S. Arimoto, M. Yoshida, M. Sekimoto, and K. Tahara, "A Riemannian-geometry approach for modeling and control of dynamics of object manipulation under constraints," *Journal of Robotics*, vol. 2009, p. 892801, 2009, (doi:10.1155/2009/892801).

[8] J. Jost, *Riemannian Geometry and Geometric Analysis*. Berlin: Springer, 2002.

[9] S. Gallot, D. Hulin, and J. Lafontaine, *Riemannian Geometory*. Berlin, Germany: Springer, 2004.

[10] S. Arimoto, *Control Theory of Non-linear Mechanical Systems: A Passivity-based and Circuit-theoretic Approach*. Oxford, UK: Oxford Univ. Press, 1996.

[11] S. H. Scott, "Apparatus for measuring and perturbing shoulder and elbow joint positions and torques during reaching," *Journal of Neuroscience Methods*, vol. 89, no. 2, pp. 119–127, 1999.

[12] V. M. Zatsiorsky, *Kinetics of Human Motion*. Champaign, IL: Human Kinetics, 2002.